A New Class of Multisection 180° Hybrids Based on Cascadable Hybrid-Ring Couplers

Kian Sen Ang, *Member, IEEE*, Yoke Choy Leong, and Chee How Lee

***Abstract*—A new class of multisection 180° hybrids is presented in this paper. It is based on the hybrid-ring coupler that has been reconfigured such that multiple sections can be conveniently cascaded together. The main limitations of the conventional hybrid-ring coupler are its limited bandwidth, large size, and the impracticably high-impedance levels required for large power-split ratios. These limitations are readily overcome using the multisection cascadable 180° hybrids. Simple design equations based on the scattering matrix and experimental verifications of the theoretical results for two-section 180° hybrids will be presented.**

***Index Terms*—Directional couplers, hybrid rings, multisection hybrids.**

I. Introduction

THE 180° hybrid-ring directional coupler is a fundamental component in microwave circuits. It performs the important function of in-phase and out-of-phase power splitting while maintaining perfectly matched ports. Compared to the 90° branch-line coupler, it has broader bandwidth [1] and the isolation between the input ports may be independent of the output termination impedances. Therefore, the 180° hybrid ring is extensively used for isolated power splitting in balanced mixers, multipliers, power amplifiers, and antenna feed networks.

Nevertheless, the conventional 180° hybrid ring has several shortcomings. It is inherently narrow-band, large in size, and it requires impracticably high-impedance line sections for large power-split ratios [2]. Although numerous techniques [2]–[9] have been proposed to overcome these limitations, most of them are not easily realizable on commonly used microstrip circuits or amenable to monolithic implementation. For example, to improve the bandwidth, March [3] replaced the $3\lambda/4$ section with a $\lambda/4$ coupled-line section, which requires very tight coupling and ground connections. Others [4]–[8] replaced the $\lambda/2$ line in the $3\lambda/4$ section with broad-band phase inverters, which cannot be implemented on microstrip circuits. Quarter-wavelength transformers have also been added to the hybrid ring for bandwidth improvement [9], which increases the overall circuit size and requires a very low impedance within the $3\lambda/4$ section. Reduced-size hybrid rings have also been implemented using $\lambda/8$ and $\lambda/6$ line sections [10], but this drastically reduces its bandwidth. To reduce the impedance levels required for high power-split ratios, Agrawal and Mikucki [2] divided the $3\lambda/4$ section into three impedance line sections. However, the impedance level required still increases with power-split ratios, which ultimately limits the achievable power-split ratio. Therefore, the quest is still on for a technique to overcome the various limitations of the hybrid ring that can be implemented on widely used microstrip circuits.

In this paper, the multisection hybrid ring is introduced to enhance the performance of the conventional hybrid ring. Although mutisection branch-line couplers and Wilkinson power dividers have been frequently employed for bandwidth improvement, multisection hybrid rings are virtually unexplored. This may be due to the fact that the conventional hybrid ring, as shown in Fig. 1(a), does not have a convenient layout for cascading multiple sections like the other two structures. However, by reconfiguring the basic hybrid ring to the layout of Fig. 1(b) with three crossovers, multiple-section hybrid rings can be readily cascaded. This reconfiguration also results in a smaller and more compact layout. In addition, the input and output ports are now conveniently located on opposite sides of the circuit instead of alternating around the conventional hybrid ring. This facilitates the ease of construction and usage of many 180° hybrid-based structures. For example, push–pull amplifiers can now be readily realized using two cascadable hybrid rings and planar monopulse comparators can be elegantly constructed using four cascadable hybrid rings. In the case of a single-balanced mixer, the local oscillator (LO) and RF inputs can be on same side of the hybrid ring, while the mixing devices are conveniently mounted on the opposite side where the IF is readily extracted.

Fig. 1(c) shows the connections required for a two-section hybrid ring using conventional hybrid rings. The output ports $3'$ and $4'$ of the first hybrid ring are, respectively, connected to the input ports $2''$ and $1''$ of the second hybrid ring. Based on this inter-connection of input and output ports of adjacent hybrid rings, more sections can be subsequently cascaded. Unfortunately, such interconnections between several hybrid rings are extremely difficult to be realized on conventional planar circuits without introducing parasitic interconnecting elements and drastically increasing circuit size. However, by employing the cascadable hybrid ring of Fig. 1(b), several hybrid rings can be directly connected to form compact multisection hybrid rings. Fig. 1(d) depicts a two-cascadable hybrid ring, which occupy about the same circuit area as the original hybrid ring. The design and performance of these cascadable hybrid rings will be presented in this paper.

II. Analysis

Based on the port assignments in Figs. 1(a) and (b), the S-parameters of the basic hybrid ring at the center frequency of op-

Manuscript received August 17, 2001.

The authors are with the Defence Science Organization National Laboratories, Singapore 118230 (e-mail: akiansen@dso.org.sg).

Publisher Item Identifier 10.1109/TMTT.2002.802328.

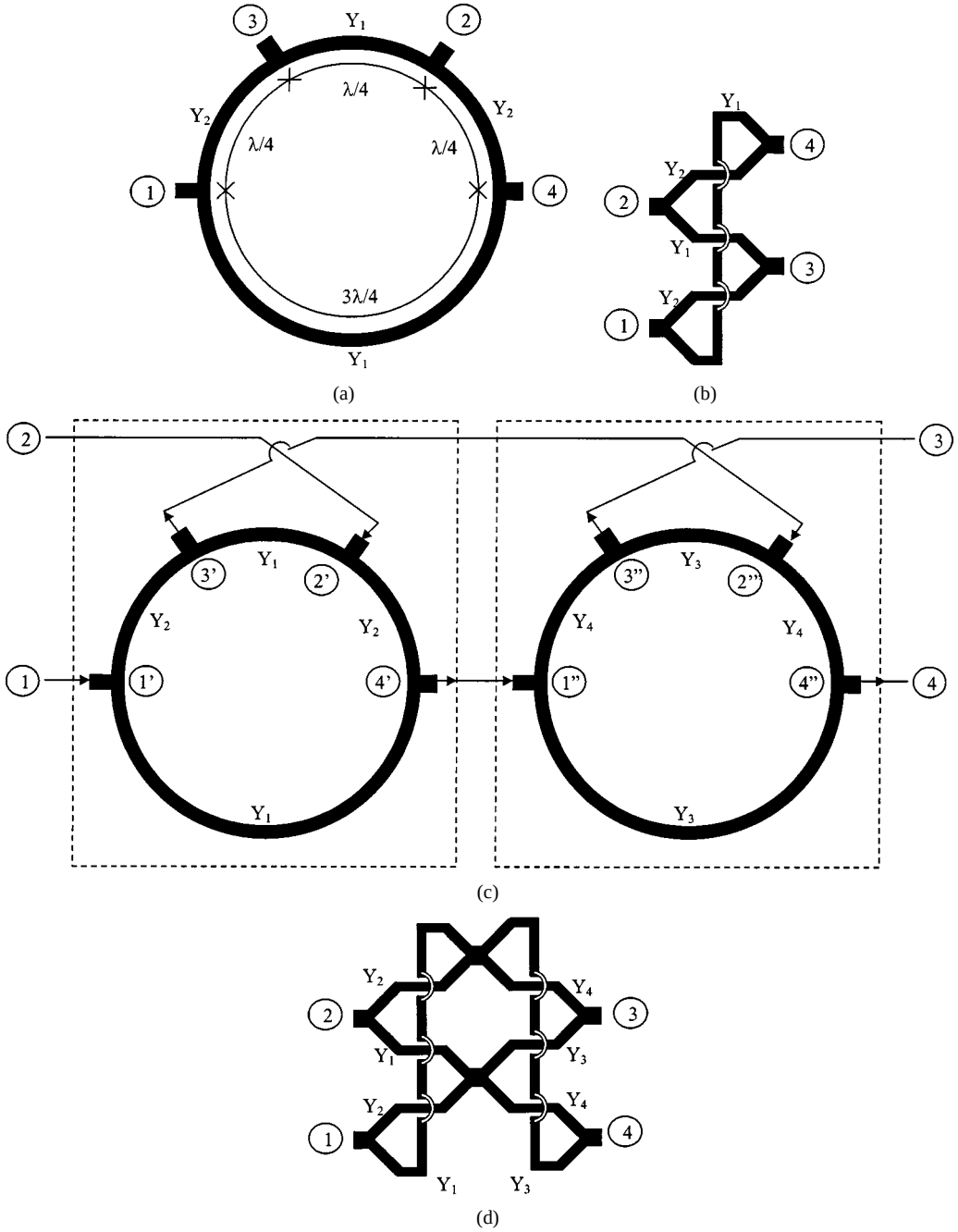

Fig. 1. (a) Conventional hybrid ring. (b) Cascadable hybrid ring. (c) Two-section hybrid ring using the conventional hybrid rings. (d) Two-section hybrid ring using cascadable hybrid rings.

eration are given by [1]

$$\begin{aligned}
S_{11} &= S_{22} = S_{33} = S_{44} = \frac{1-\left(Y_1^2+Y_2^2\right)}{1+Y_1^2+Y_2^2} \\
S_{21} &= S_{43} = 0 \\
S_{31} &= -j\frac{2Y_2}{1+Y_1^2+Y_2^2} \\
S_{41} &= j\frac{2Y_1}{1+Y_1^2+Y_2^2} \\
S_{32} &= -j\frac{2Y_1}{1+Y_1^2+Y_2^2} \\
S_{42} &= -j\frac{2Y_2}{1+Y_1^2+Y_2^2}.
\end{aligned} \tag{1}$$

Equation (1) shows that the in-phase and out-of-phase power-splitting characteristics, as well as the isolation of the input and output ports are independent of the admittances Y_1 and Y_2. However, for all the ports to be perfectly matched, we require

$$Y_1^2 + Y_2^2 = 1. \tag{2}$$

When (2) is satisfied

$$\begin{aligned}
S_{31} &= -jY_2 = -\frac{j}{Z_2} \\
S_{41} &= jY_1 = \frac{j}{Z_1}.
\end{aligned} \tag{3}$$

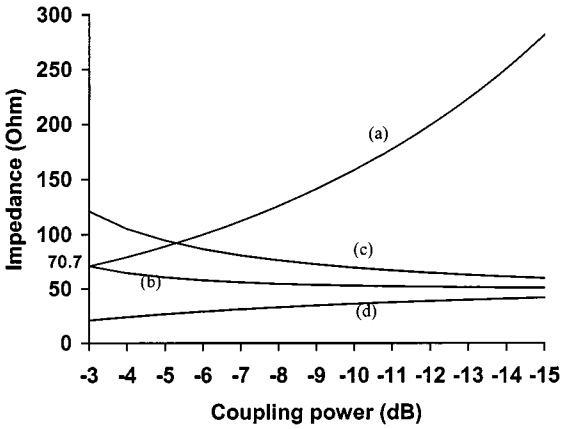

Fig. 2. Impedance levels required for various coupling ratios for: (a) Z_2 in single-section hybrid ring, (b) Z_1 in single-section hybrid ring, (c) Z_2' in two-section hybrid ring with $Z_1' = 50\ \Omega$, and (d) Z_1' in two-section hybrid ring with $Z_2' = 50\ \Omega$.

Equation (3) depicts the design equations for the single-stage hybrid ring with arbitrary power-split ratios. The impedance values required for Z_1 and Z_2 for various coupling levels assuming 50-Ω port terminations are shown in Fig. 2(a) and (b). It can be seen that $Z_1 = Z_2 = 70.7\ \Omega$ for 3-dB coupling and Z_1 decreases toward 50 Ω, while Z_2 increases to exceedingly high values for high coupling ratios.

Considering the two-section hybrid rings in Fig. 1(c) and (d) as a cascade of two four-port networks, the overall S-matrix can be derived by using the multiport connection method [11]. The results are as follows:

$$\begin{aligned}
S_{11} &= S_{22} = -S_{33} = -S_{44} = \frac{\left(Y_3^2 + Y_4^2\right) - \left(Y_1^2 + Y_2^2\right)}{Y_1^2 + Y_2^2 + Y_3^2 + Y_4^2} \\
S_{21} &= S_{43} = 0 \\
S_{31} &= -\frac{2\left(Y_1 Y_3 + Y_2 Y_4\right)}{Y_1^2 + Y_2^2 + Y_3^2 + Y_4^2} \\
S_{41} &= \frac{2\left(Y_1 Y_4 - Y_2 Y_3\right)}{Y_1^2 + Y_2^2 + Y_3^2 + Y_4^2} \\
S_{32} &= -\frac{2\left(Y_1 Y_4 - Y_2 Y_3\right)}{Y_1^2 + Y_2^2 + Y_3^2 + Y_4^2} \\
S_{42} &= -\frac{2\left(Y_1 Y_3 + Y_2 Y_4\right)}{Y_1^2 + Y_2^2 + Y_3^2 + Y_4^2}.
\end{aligned} \tag{4}$$

From (4), we can see that the two-section hybrid ring has the same in-phase and out-of-phase power-splitting and isolation properties as the basic hybrid ring.

If we consider the symmetrical case where $Y_3 = Y_2$ and $Y_4 = Y_1$, all the ports will be perfectly matched and the transmission S-parameters will be given by

$$\begin{aligned}
S_{31} &= -\frac{2\left(\frac{Y_2}{Y_1}\right)}{1 + \left(\frac{Y_2}{Y_1}\right)^2} = -\frac{2\left(\frac{Z_1'}{Z_2'}\right)}{1 + \left(\frac{Z_1'}{Z_2'}\right)^2} \\
S_{41} &= \frac{1 - \left(\frac{Y_2}{Y_1}\right)^2}{1 + \left(\frac{Y_2}{Y_1}\right)^2} = \frac{1 - \left(\frac{Z_1'}{Z_2'}\right)^2}{1 + \left(\frac{Z_1'}{Z_2'}\right)^2}.
\end{aligned} \tag{5}$$

Therefore, the power-split ratio of the two-section hybrid-ring coupler depends on the ratio of impedances Z_1' and Z_2' instead of their absolute values as in the single-section hybrid ring. Fig. 2(c) and (d) shows the impedance levels required for Z_1' and Z_2' when one of them is set to a convenient impedance of 50 Ω. If Z_1' is set to 50 Ω, the required value for Z_2' is 121 Ω for 3-dB coupling and decreases toward 50 Ω with increasing coupling ratios. If Z_2' is set to 50 Ω instead, the required impedance for Z_1' is 21 Ω for 3-dB coupling and increases toward 50 Ω with increasing coupling ratios. Therefore, the two-section hybrid ring can be realized with a wide range of highly realizable impedance levels for high power-split ratios. This alleviates the serious limitation of realizability that prevails for conventional hybrid rings for high power-split ratios.

III. Experimental Results

Practical implementation of the cascadable hybrid rings requires several crossovers. These may cause undesirable coupling, mismatch, and other parasitic effects. However, this effects can be minimized by ensuring that the lengths of the crossovers are sufficiently small compared to the $\lambda/4$ line sections. To demonstrate the proposed technique and validate the analytical results, three 180° hybrids were designed. The photographs of the fabricated hybrid rings are shown in Fig. 3(a)–(c). These circuits were realized using microstrips on a low-cost FR-4 board where the traces are defined by a T-tech printed circuit board (PCB) router. The crossovers were implemented by soldering stripes of copper tape across the microstrip traces.

The single-stage cascadable 3-dB hybrid ring shown in Fig. 3(a) is fabricated first to verify its performance. Fig. 4 shows the measured coupling parameters, S_{32} and S_{42}. Also shown are the simulation results using Agilent's ADS software,[1] based on ideal transmission lines with $Z_1 = 70.7\ \Omega$ and $Z_2 = 70.7\ \Omega$. The discrepancies between simulation and measurement at higher frequencies can be attributed to the microstrip losses that are not accounted for in the simulations. Equal power split is achieved around 2.4 GHz over a limited bandwidth. The measured insertion loss is approximately 0.4 dB for the single-stage hybrid ring. The phase balance between the difference ports (S_{31}/S_{41}) is shown in Fig. 5. Perfect out-of-phase (180°) power split is only obtained at the center frequency of 2.4 GHz. Therefore, the single-section cascadable hybrid ring exhibits the familiar narrow-band characteristics of a conventional hybrid ring.

The two-stage cascadable 3-dB hybrid ring shown in Fig. 3(b) is then implemented with $Z_1' = 50\,\Omega$ and $Z_2' = 120\,\Omega$. The simulated and measured coupling parameters are shown in Fig. 6. Equal power split is now achieved over a broader bandwidth from 1.6 to 2.8 GHz. The measured insertion loss has increased proportionally to approximately 0.8 dB for the two-section hybrid ring. The phase balance between the difference ports is $\pm 10°$ within the passband, as shown in Fig. 7. Therefore, considerable bandwidth improvement has been achieved by employing the two-section hybrid ring.

[1]Advanced Design System, ver. 1.3, Agilent Technol., Palo Alto, CA, 1999.

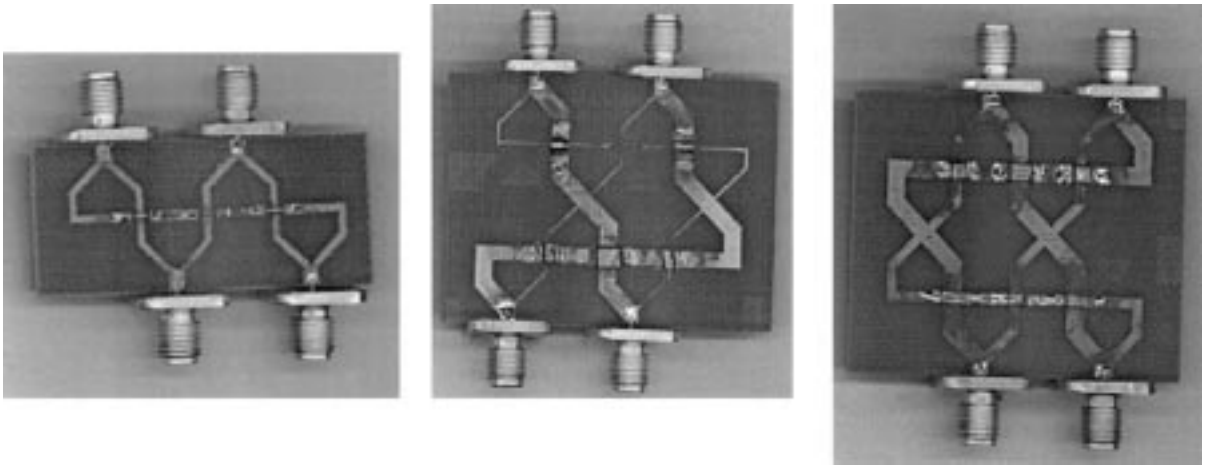

(a) (b) (c)

Fig. 3. Fabricated cascadable hybrid rings. (a) Single-section 3-dB hybrid (b) Two-section 3-dB hybrid. (c) Two-section 7-dB hybrid.

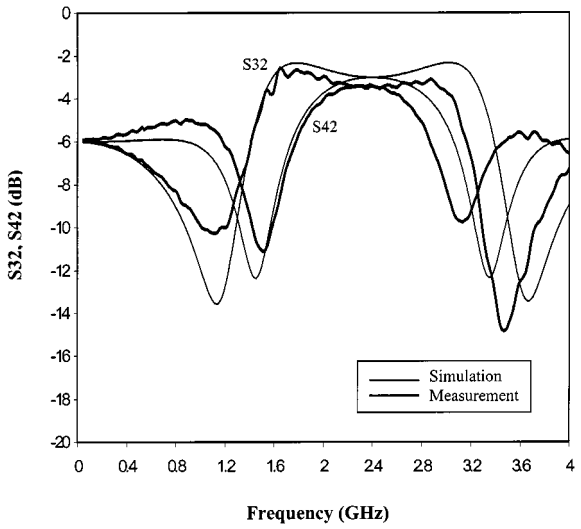

Fig. 4. Coupling parameters of the single-section 3-dB cascadable hybrid ring.

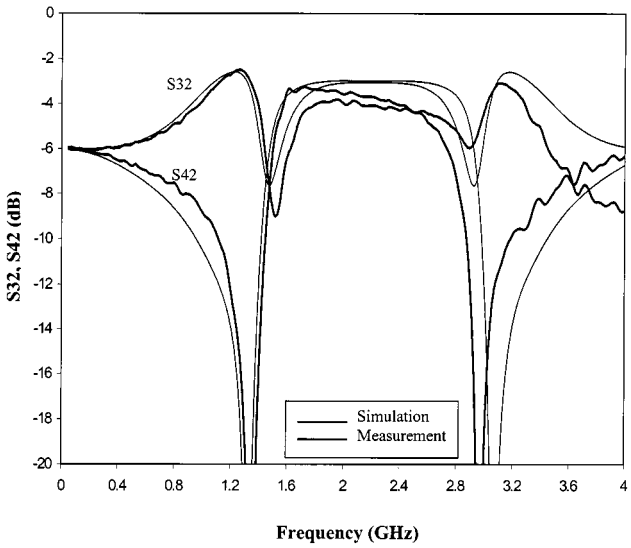

Fig. 6. Coupling parameters of the two-section 3-dB cascadable hybrid ring.

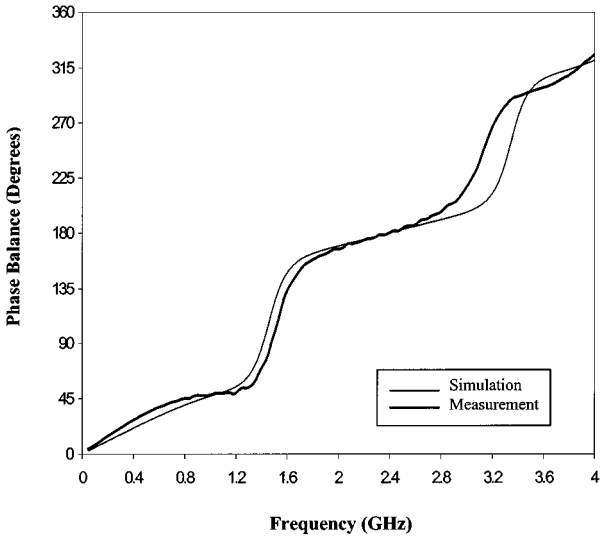

Fig. 5. Phase imbalance between the difference ports of the single-section 3-dB cascadable hybrid ring.

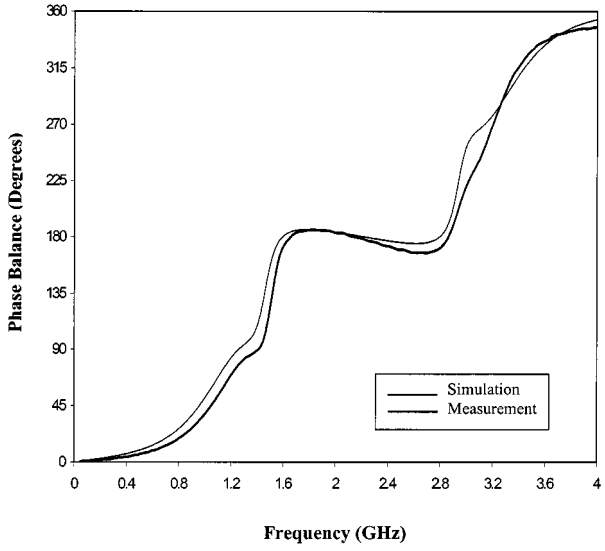

Fig. 7. Phase balance between the difference ports of the two-section 3-dB cascadable hybrid ring.

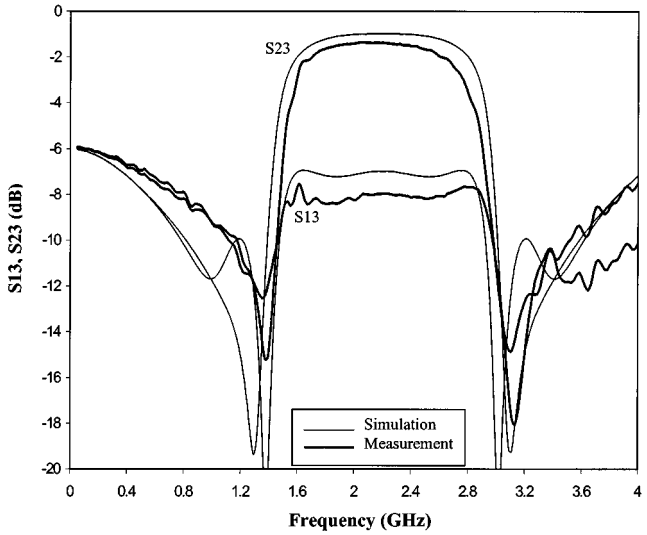

Fig. 8. Coupling parameters of the two-section 7-dB cascadable hybrid ring.

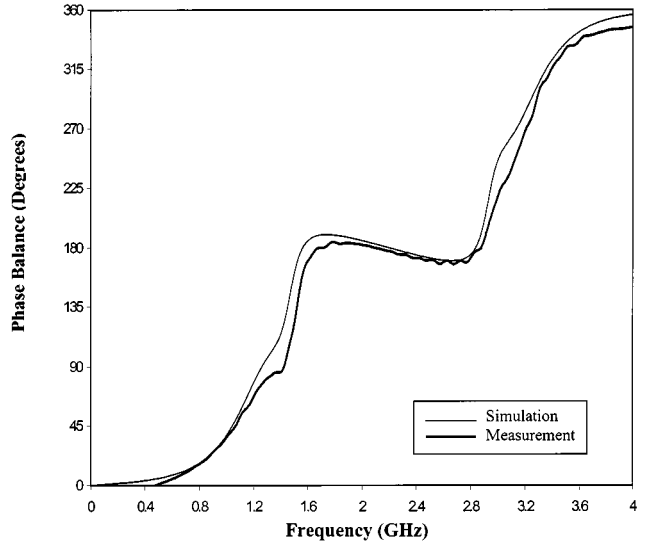

Fig. 9. Phase balance between the difference ports of the two-section 7-dB cascadable hybrid ring.

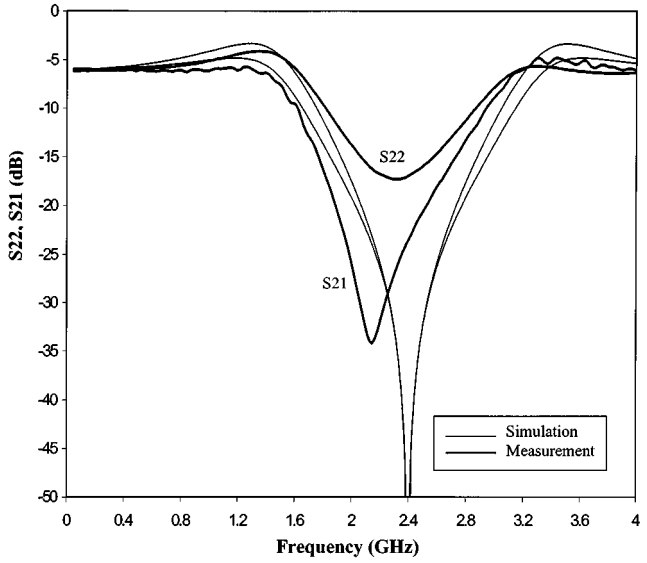

Fig. 10. Isolation and return losses of the single-section 3-dB cascadable hybrid ring.

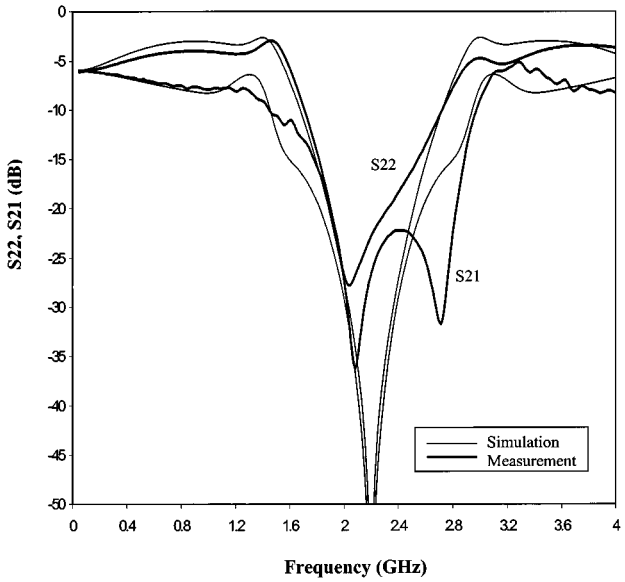

Fig. 11. Isolation and return losses of the two-section 7-dB cascadable hybrid ring.

Finally, a two-stage 7-dB hybrid-ring coupler shown in Fig. 3(c) is implemented with $Z_1' = 50\,\Omega$ and $Z_2' = 81\,\Omega$ to demonstrate unequal power split. The measured coupling parameters shown in Fig. 8 is close to the designed value, taking into account the 0.8-dB insertion loss for two-section hybrid rings. Similarly, a phase balance of $\pm 10^\circ$ is achieved from 1.6 to 2.8 GHz, as shown in Fig. 9.

Also measured are the isolation and return losses of the various cascadable hybrids. The typical isolations and return losses for the single- and two-section 3-dB hybrids are shown in Figs. 10 and 11, respectively. Over 20-dB isolation is generally achieved within the passbands, while the return loss is approximately 15 dB.

IV. Conclusion

This paper has demonstrated that multisection 180° hybrids can be realized by reconfiguring the basic hybrid ring. The resulting multisection hybrids offer improvement in bandwidth, reduction in size, and alleviate the realizability problem that prevails conventional hybrid rings with high power-split ratios. The broad-band nature of the amplitude and phase balance achieved for the difference ports also shows that these hybrids can be used in place of baluns frequently found in balanced circuits. This will provide simultaneously matched and isolated ports, which cannot be obtained from three-port lossless baluns [12]. Moreover, baluns are susceptible to imbalances caused by unequal even- and odd-mode phase velocities of the microstrip coupled-line sections in the balun. Finally, similar to multisection (90°) branch-line couplers and (0°) Wilkinson power dividers, more sections of the basic hybrid ring may be cascaded to synthesize specific broad-band Butterworth or Chebyshev responses [7]. Therefore, with the development of these cascadable hybrid rings, there is a complete set of multisection hybrids for broad-band power splitting with 0°, 90°, as well as 180° phase difference.

Acknowledgment

The authors would like to thank K. K. Ang, DSO National Laboratories, Singapore, for his technical support in the circuit fabrication.

REFERENCES

[1] C. Y. Pon, "Hybrid-ring directional coupler for arbitrary power divisions," *IRE Trans. Microwave Theory Tech.*, vol. MTT-9, pp. 529–535, Nov. 1961.

[2] A. K. Agrawal and G. F. Mikucki, "A printed circuit hybrid-ring directional coupler for arbitrary power divisions," *IEEE Trans. Microwave Theory Tech.*, vol. MTT-34, pp. 1401–1407, Dec. 1986.

[3] S. March, "A wideband stripline hybrid ring," *IEEE Trans. Microwave Theory Tech.*, vol. MTT-16, p. 361, June 1968.

[4] S. Rehnmark, "Wide-band balanced line microwave hybrids," *IEEE Trans. Microwave Theory Tech.*, vol. MTT-25, pp. 825–830, Oct. 1977.

[5] M. H. Murgulescu, E. Penard, and I. Zaquine, "Design formulas for generalized 180° hybrid ring couplers," *Electron. Lett.*, vol. 30, no. 7, Mar. 1994.

[6] T. Wang and K. Wu, "Size-reduction and band-broadening design technique of uniplanar hybrid ring coupler using phase inverter for M(H)MIC'S," *IEEE Trans. Microwave Theory Tech.*, vol. 47, pp. 198–206, Feb. 1999.

[7] C. Y. Chang and C. C. Yang, "A novel broad-band Chebyshev-response rat-race ring coupler," *IEEE Trans. Microwave Theory Tech.*, vol. 47, pp. 455–462, Apr. 1999.

[8] C.-W. Kao and C. H. Chen, "Novel uniplanar 180° hybrid-ring couplers with spiral-type phase inverters," *IEEE Microwave Guided Wave Lett.*, vol. 10, pp. 412–414, Oct. 2000.

[9] D. I. Kim and Y. Naito, "Broad-band design of improved hybrid ring 3-dB directional couplers," *IEEE Trans. Microwave Theory Tech.*, vol. MTT-30, pp. 2040–2046, Nov. 1982.

[10] D. I. Kim and G. S. Yang, "Design of new hybrid-ring directional coupler using $\lambda/8$ or $\lambda/6$ sections," *IEEE Trans. Microwave Theory Tech.*, vol. 39, pp. 1779–1783, Oct. 1991.

[11] J. A. Dobrowolski, *Introduction to Computer Methods for Microwave Circuit Analysis and Design*. Norwood, MA: Artech House, 1991, pp. 81–90.

[12] K. S. Ang and I. D. Robertson, "Analysis and design of impedance-transforming planar Marchand baluns," *IEEE Trans. Microwave Theory Tech.*, vol. 49, pp. 402–406, Feb. 2001.

Kian Sen Ang (M'02) was born in Singapore, in 1969. He received the B.Eng. degree from the National University of Singapore, Singapore, in 1994, and the Ph.D. degree from the University of Surrey, Surrey, U.K., in 2000.

In 1994, he joined the Defence Science Organization (DSO) National Laboratories, Singapore, as a Research Engineer involved in microwave circuit and sub-system designs. He is currently a Senior Member of Technical Staff with the DSO National Laboratories. His research interests include design, analysis, and measurement of novel microwave circuits including monolithic integrated circuits. He has authored over 20 publications in this area and was a contributing author of *RFIC and MMIC Design and Technology* (London, U.K.: IEE Press, 2001).

Yoke Choy Leong received the B.Eng. (with honors) and M.Sc. degrees from the National University of Singapore, Singapore, in 1991 and 1995, respectively, and the Ph.D. degree from the University of Massachusetts at Amherst, in 2000.

Since 1991, he has been with the Defence Science Organization (DSO) National Laboratories, Singapore, where he is involved in the area of microwave component and system design. His research interest is in microwave/millimeter-wave monolithic microwave integrated circuit (MMIC) design and modeling, analysis, and synthesis of novel passive structures.

Chee How Lee was born in Singapore, in 1975. He received the M.Eng. degree from the Imperial College of Science, Technology and Medicine, London, U.K., in 1998.

Since 2001, he has been an Engineer with Defence Science Organization (DSO) National Laboratories, Singapore, where he has been involved in microwave component and sub-system design. His research interest is in the design, analysis, and synthesis of microwave MMIC and novel passive structures.